University of Alberta

Well Site Selection Algorithm Considering Geological, Economical and Engineering Constraints

By

Bujin Wang

A thesis submitted to the Faculty of Graduate Studies and Research in partial fulfillment of the requirements for the degree of **Master of Science**

in

Petroleum Engineering

Department of Civil and Environmental Engineering

Edmonton, Alberta

Spring 2001

National Library of Canada
Acquisitions and Bibliographic Services
395 Wellington Street
Ottawa ON K1A 0N4
Canada

Bibliothèque nationale du Canada
Acquisitions et services bibliographiques
395, rue Wellington
Ottawa ON K1A 0N4
Canada

Your file Votre référence

Our file Notre référence

The author has granted a non-exclusive licence allowing the National Library of Canada to reproduce, loan, distribute or sell copies of this thesis in microform, paper or electronic formats.

L'auteur a accordé une licence non exclusive permettant à la Bibliothèque nationale du Canada de reproduire, prêter, distribuer ou vendre des copies de cette thèse sous la forme de microfiche/film, de reproduction sur papier ou sur format électronique.

The author retains ownership of the copyright in this thesis. Neither the thesis nor substantial extracts from it may be printed or otherwise reproduced without the author's permission.

L'auteur conserve la propriété du droit d'auteur qui protège cette thèse. Ni la thèse ni des extraits substantiels de celle-ci ne doivent être imprimés ou autrement reproduits sans son autorisation.

0-612-60512-4

Canada

University of Alberta

Library Release Form

Name of Author: Bujin Wang

Title of Thesis: Well Site Selection Algorithm Considering Geological, Economical and Engineering Constraints

Degree: Master of Science

Year this Degree Granted: 2001

Permission is hereby granted to the University of Alberta Library to reproduce copies of this thesis and to lend or sell such copies for private, scholarly or scientific purpose only.

The author reserves all other publication and other rights in association with the copyright in the thesis, and except as herein before provided, neither the thesis nor any substantial portion thereof may be printed or otherwise reproduced in any material form whatever without the author's prior written permission.

148 Michener park,
Edmonton, Alberta,
Canada T6H 4M4

Dec 22, 2000

University of Alberta

Faculty of Graduate Studies and Research

The undersigned certify that they have read, and recommend to the Faculty of Graduate Studies and Research for acceptance, a thesis entitled **Well Site Selection Algorithm Considering Geological, Economical and Engineering Constraints** submitted by **Bujin Wang** in partial fulfillment of the requirements for the degree of **Master of Science in petroleum engineering.**

Dr. Clayton V. Deutsch

Dr. Mingjian Zuo

Dr. Ergun Kuru

Abstract

Well placement decisions must be made in the face of geological, engineering and economic constraints. Some of these constraints include (1) maximum intersection of connected volumes of high quality reservoir, (2) avoidance of fluid contacts that could cause early breakthrough and reduce productivity, (3) maximum pore volume that could be drained, (4) compliance with existing wells as well as physical drilling constraints.

A fast and efficient iterative algorithm based on simulated annealing is proposed for well planning subject to multiple constraints and uncertainty in the reservoir model. Connected volume and pore volume are used as the main criteria in our examples. Several examples from simple to real reservoir models for placement of different number of wells and well types are tested and presented.

Acknowledgements

First, a big thanks to my supervisor Clayton Deutsch who makes me to devote in this thesis and have it done. And thanks for the opportunity to work with you and the other CCG folks at University of Alberta. There have been precious few times in my life when I've actually been excited about going to work on the computer!

Thanks to my wife and little daughter—"I have to work on my thesis." is always my excuse for not staying with you.

I must also thank everyone associated with my thesis. Dr. MingJian Zuo and Dr. Ergun Kuru spent their precious time to review my thesis. Faculty of Graduate Studies and Research helped with me on different stages of my graduation.

Finally, I wish to thank Scot Evans, Dan Colvin and Dr. Genbao Shi at Landmark Graphics Co. for their help on my research.

Edmonton, Alberta

Bujin Wang December 21, 2000

Table of Contents

Table of Contents

Abstract

Introduction 1

1 Well Site Selection Algorithm 5
- 1.1 Grid Topology and Reservoir Definition . . . 5
- 1.2 Well Trajectory Definition . . . 6
- 1.3 Constraints . . . 9
  - 1.3.1 Well Type: Vertical, Horizontal, and Deviated . . . 9
  - 1.3.2 Static Connectivity(Geo-Objects) . . . 9
  - 1.3.3 Hydrocarbon Pore Volume . . . 12
- 1.4 Optimization Considerations . . . 14
  - 1.4.1 Multiple Geostatistical Realizations . . . 14
  - 1.4.2 Interaction Between Wells . . . 14
- 1.5 Optimization Algorithm . . . 15
- 1.6 Flow Chart . . . 18
- 1.7 Software Engineering . . . 19

2 Testing and Validation 23
- 2.1 Homogeneous Model . . . 23
- 2.2 Heterogeneous Model . . . 25
- 2.3 3-D Heterogeneous Model . . . 32
- 2.4 Exhaustive Example . . . 32
- 2.5 Multiple Realizations . . . 35
- 2.6 A Real Example With Multiple Well Types . . . 42

3 Limitations and Future Work **44**
3.1 Additional Constraints 44
3.1.1 Productivity 44
3.1.2 More Complex Geological Structure 45
3.1.3 Fluid Contacts 45
3.1.4 Tortuosity 46
3.1.5 Drilling Constraints 47
3.2 Combining Component Objective Functions 48
3.3 Optimization Algorithm 49
3.3.1 Local Minima 49
3.3.2 Number of Iterations 50
3.4 Summary and Conclusions 51

Bibliography **52**

Introduction

Introduction

Reservoir decision making depends primarily on predicted performance at possible well locations. The task of the reservoir development team is to choose well locations and production strategies to maximize production at minimum cost and meet other varied corporate objectives. Flow simulation provides a rigorous approach to predict reservoir behavior.

In order to optimize well placement, a large number of well configurations, including location, and orientation must be examined. The time needed for reservoir simulation makes it impossible to evaluate all possible combinations. Additionally, the current trend of introducing multiple geostatistical realizations into reservoir decision making, to represent the uncertainty in the geological description, increases problem. A fast technique to evaluate many possible well configurations and identify the optimal locations for further flow studies is needed. The technique must consider geological uncertainty represented by geostatistical realizations.

Stochastic realizations have long been used to capture the uncertainty in different reservoir modeling stages. In papers [31, 20, 18], geostatistical modeling of uncertainty has been noticed and calibrated in structural modeling. Deutsch introduced a program(FLUVSIM[10]) to model Fluvial Depositional Systems[11] using Object-Based

Stochastic techniques. In 1993, Georgsen[28] used Fibre Processes and Gaussian Random Functions for Modeling Fluvial Reservoirs. In production stage, geostatistical modeling is also widely used[21, 29, 2]. Uncertainty has also been introduced in property modeling[4, 14].

Ranking realizations, a technique which could be used to reduce the number of realizations that must be considered, can be found in a number of papers [31, 9, 15, 25]; However , there is a large number of well positions to be evaluated for the reduced number of realizations .

In well planning, 3D geostatistical models representing reservoir character have been used to assess the production from planned wells. In 1995 Goggin et al. [13] reported a well-position optimization method based on statistics. Horizontal well locations has been optimized by maximizing recovery and minimizing the number of wells. Structural and stratigraphic information were combined with processed log data to construct the model. No uncertainty has been considered.

Gutteridge et al.[15] took the application of 3D geological reservoir models forward from basic well planning, to a screening and ranking of multiple well path options based on quality of connection to volumes of net sand and on instantaneous productivity index. Quality factor maps were used in their research as potential well positions, and then well paths were ranked in order to obtain optimal well sites. They took advantage of what they called "shared earth model", the model generated by latest 3D modeling packages. Uncertainty was not considered in that work.

In 1996, D. Seifert [27] generated geological 3-D stochastic reservoir models by integrating reservoir specific and outcrop analogue data into a hybrid deterministic-stochastic model. The model provides the basis for the determination of the optimum

well trajectories and the subsequent risks of their success. In his work, both horizontal wells and inclined wells were evaluated over multiple realization. To Optimize clustered well trajectories was the main concern.

"Integer Programming Optimization" was also applied as an automatic well selection method by S. Vasantharajan et al. [30]. In this work, quality map was used as input to the well site selection.

P. Cruz et.al. [3] presents an approach to incorporate geological uncertainty in the selection of the best production scenario among a set of predefined scenarios. A quality map which calibrates "how good the area is for production" is constructed by calculating well production assuming no other wells in the reservoir. Interaction between wells has been ignored due to heavy CPU-cost of simulators.

There are different kinds of constraints that need to be taken into account when planning wells. These constraints include geology, engineering and economic constrains. There is always uncertainty in the geological model used for well planning. When planning multiple wells, interaction between wells is important.

In this thesis, an integrated well site selection algorithm is proposed to take care of the parameters encountered both in exploration and development stage, such as the geo-objects a well trajectory may perforate, connected volume, various lithologic properties of reservoir rock like porosity, permeability and geologic structure and structural position. Deviated wells, vertical wells and horizontal wells are frequently drilled to enhance production. The algorithm accounts for interactions between planned wells and pre-existing wells.

The well site selection algorithm intends to find good well configurations, but sometimes called "optimal" for the procedure used. Simply because it is easier to be

called.

Various constraints can be simultaneously considered as component objective functions. These components must be combined into a single objective function to be minimized. A technique of weighting component objective functions introduced by Deutsch [6] is used here to take care of individual significance.

The algorithm was first implemented in Visual Basic[33, 32] with an easy-to-use interface. Several examples generated by this algorithm are shown. The first implementation could only optimize vertical wells and to maximize connected volume. A Second implementation in Java within Landmark Graphics Co. development environment was coded. A popular topology in petroleum industry called "SGrid" from GOCAD is employed to represent our reservoir model. An industry standard user interface is designed to allow users to easily pick initial configurations and set parameters. In this second version, deviated wells, horizontal wells and vertical wells are able to be optimized together and pore volume is used as the criteria. An example with real reservoir model will be presented.

Chapter 1

Well Site Selection Algorithm

1.1 Grid Topology and Reservoir Definition

Our topology follows GOCAD's[1] SGrid format. SGrid is a sophisticated 3-D grid in which the positions of nodes are controlled by surfaces, lines, and points. The grid is regular in parametric (U,V,W) coordinates, but irregular in spatial (X,Y,Z) coordinates.

In spatial (X,Y,Z) coordinate system, the cell is delineated by its 8 apices and their properties. These 8 apices define an irregular grid, that is, they could be any shape. These apices could be separated with other grids due to faults.

In SGrid, faults, facies and layers can be represented by TFace and TSurf. The location or coordinates information could be extracted once the model is loaded. Figure 1.1 shows one layer of SGrid. Note that faults cause the 'broken' surface of the model. Layers are numbered from bottom to top with no overlap of cells. Cells may share or not share faces, edges or apices, but never overlap each other.

In well planning, well trajectories must ultimately intersect the reservoir. The 3-D points on the trajectories must be checked to determine whether they are inside

Figure 1.1: One layer in a SGrid

the reservoir or not. In order to determine whether a 3-D point is inside the SGrid or not, a conversion from spatial coordinates to parametric(U,V,W) coordinates should be used. If the point is inside, the counterpart in parametric coordinates should be all between (0,1). SGrid will be used to represent our geologic and property model.

1.2 Well Trajectory Definition

Well path is a 1-D trajectory defined by a sequential set of coordinate locations $\{(x_i, y_i, z_i), i = 1, ..., N\}$, where N is the number of points defining the path. The complete trajectory path can be interpolated linearly or using splines based on the N control points. Figure 1.2 shows how a common well trajectory is defined with four

Figure 1.2: Definition of a well path with 4 control points

points.

We define two-point line segments as our objective "well". In practice, these line segments form a complete well trajectory. If the line segments follow a vertical line, then, it is called a vertical well. If the straight line is deviated from vertical line, it is called an inclined well. When it is horizontal, a horizontal well path forms. Figure 1.3 shows the three different wells.

Well types defined above can be differentiated by parameters like dip and azimuth. For a vertical well, dip equals to zero; for a horizontal well, dip equals to 90 degrees. The dips for deviated wells are in between this range.

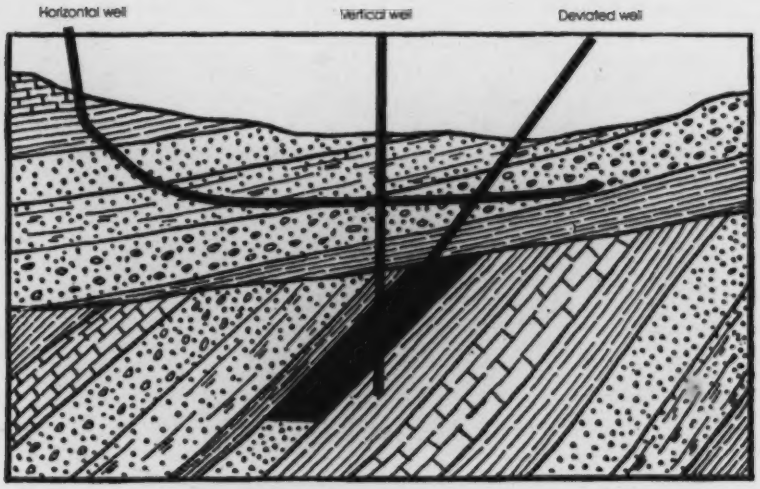

Figure 1.3: Three well types: horizontal, vertical and deviated wells

Realistically, vertical and horizontal wells may not perfectly have 0 or 90 degree in dip, but allow some tolerance. A range of 2 degrees is very common as used in Landmark Graphics Co. Under this assumption, a well with dip within $[0, 2]$ is defined as a vertical well ; a well with dip within $[88, 90]$ is a horizontal well. The dip for a deviated well, then, takes what was left after the range of vertical well and horizontal well, in this case, dip is between$(2, 88)$.

For a deviated and horizontal wells, the azimuth is another controlling parameter. For azimuth, the angle from the north direction with clockwise is positive and counterclockwise is negative. Both horizontal well and deviated well have azimuth. But, since a vertical well is perpendicular, there is no azimuth defined.

1.3 Constraints

1.3.1 Well Type: Vertical, Horizontal, and Deviated

For vertical wells, there is no tilt and rotation movement. It can only be moved areally. A horizontal well can be rotated. Deviated or inclined well could take any types of movement defined as *move*, *upDown*, *tilt* and *turnAround*. An Object Oriented design will be described later to implement these behaviours.

1.3.2 Static Connectivity(Geo-Objects)

A reservoir consists of connected regions, which we wish to produce with the fewest number of wells in the best locations. The different connected regions in a reservoir are called "geo-objects". Each geo-object is a collection of net (reservoir quality) cells connected together but disconnected from the others. Figure 1.4 illustrates three geo-objects; the volume outside of these objects is non-reservoir. By convention, in the presence of n geo-objects, the geo-objects are sorted according to their sizes. The largest is labeled 1 and the smallest is labeled n.

Deutsch [5] provides details on the calculation of geo-object connectivity. The program for geo-object calculation is integrated into the program for well site selection; the user inputs are the facies, porosity, and permeability models required to establish the reservoir regions that are "net" reservoir quality.

The connected volume (CV) to a well location represents the reservoir volume that can be drained by a well, that is, the reservoir volume that is reservoir quality *and* connected to the well location *and* within the drainage radius of the well. The

connected volume depends on the geo-objects intersected by the well and their distribution within the drainage radius. In presence of multiple geostatistical realizations, the average or expected value of the connected volume for a well location may be determined.

Let Ω represent the set of all cells within the drainage radius of the well. The variable, $i(u, u_w)$ represents the probability of a location being connected to the well location. That is,

$$i(u, u_w) = \begin{cases} 1, \text{if location } u \text{ is connnected to well at location } u_w \\ 0, \text{otherwise} \end{cases} \tag{1.3.1}$$

When multiple well locations are considered, every cell $i(u, u_w)$ in its cell set Ω will be checked and set according to 1.3.1. This is an iterative process which will go through all the well locations u_w. Note that there are some cells in Ω which may be drained by other wells if wells are close. In this case, indicator $i(u, u_w)$ for these cells u actually "have been" or "will be" set to 1 because they are inside the drainage area.

The connected volume for well u_w is the indicator-weighted sum of all cells in the drainage radius:

$$CV_w = \sum_{u \in \Omega} V_{cw} \times i(u; u_w), \text{ where } V_{cw} \text{ is volume of a cell} \tag{1.3.2}$$

A single well trajectory can intersect several geo-objects simultaneously. The connected volumes is the sum of all the cell volume that fit the criteria specified above.

Figure 1.4 shows a schematic example. The cells hatched are to be counted in the connected volume of the well. The cells outside the drainage radius, such as the left part of geo-object 2 in Figure 1.4, is not counted in the connected volume. Since

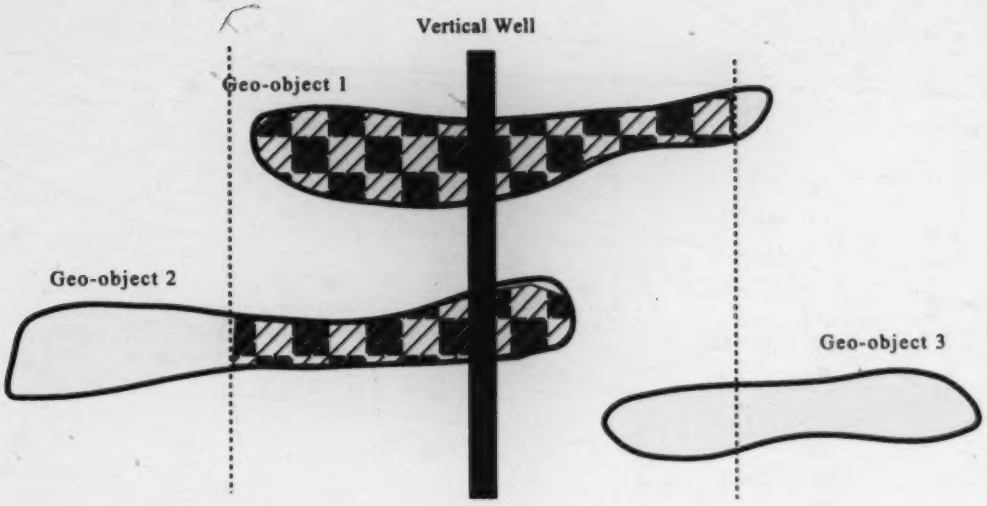

Figure 1.4: Schematic illustration of geo-objects and connected volume to a well location. The dash lines represent the drainage radius.

the well doesn't intersect geo-object 3, although some of the cells of geo-object 3 are within the drainage radius, this geo-object is not considered.

For the multiple well configuration, we need to calculate the total CV of all the wells, the cumulative connected volume (CCV):

$$CCV = \sum_{w=1}^{n_w} CV_w = V_c \sum_{w=1}^{n_w} \sum_{u \in \Omega} i(u; u_w), \ n_w \text{ is number of wells} \tag{1.3.3}$$

The CCV can be used as a criteria for well positioning. For the same number of wells, we would prefer the well configuration with the greatest CCV.

The simplest case is when only one well location is to be found. The CV for all candidate locations can be calculated and the well will be placed at the site with the maximum connected volume. This procedure could be repeated sequentially to place multiple wells; however, this will not, in general, achieve the maximum CCV. Figure 1.5 illustrates the concept with a simple example. The multiple-well case is

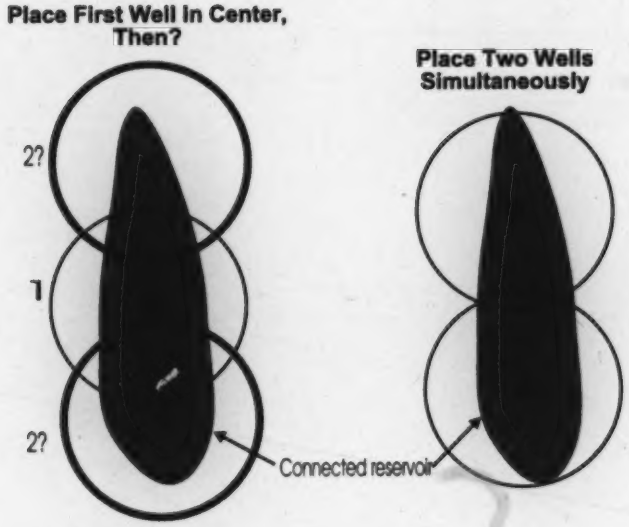

Figure 1.5: Schematic illustration showing that picking the wells sequentially (without regard for other wells) would be suboptimal.

complicated because the number of combinations to consider is large.

1.3.3 Hydrocarbon Pore Volume

Consider a reservoir which is initially filled with liquid oil. The oil volume in the reservoir(oil in place) Θ is

$$\Theta = V\phi(1 - S_{wc}) \tag{1.3.4}$$

where V is the new bulk volume of the reservoir rock, ϕ is the porosity or volume fraction of the rock which is porous and S_{wc} is the connate or irreducible water saturation and is expressed as a fraction of the pore volume.

The product $V\phi$ is called the pore volume (PV) and is the total volume in the reservoir which can be occupied by fluids. Similarly, the product $V\phi(1-S_{wc})$ is called

the hydrocarbon pore volume ($HCPV$) and is the total reservoir volume which can be filled with hydrocarbons such as oil, gas or both.

However, not all the volume of hydrocarbons can be produced or drained. Usually, if the hydrocarbon volume is too far from the well bore, the well fails to obtain the amount of volume. Only the portion within given area can be produced. We define this area as "effective area". Effective area is the area near well bore(s) in which the hydrocarbon volume could be produced or drained with the well(s). For a homogeneous reservoir, the effective area is a round area with effective distance as its radius. For heterogeneous reservoir, an arbitrary effective area is defined to account for the directional differences.If the effective area is regular shape, for example, a circle, then a "effective distance" is defined as the distance within which the hydrocarbons volume can be produced or drained with the well(s).

Similar to the definition of cumulative connected volume, we define the cumulative hydrocarbon pore volume. Let Ω represent the set of all cells within the drainage radius of the well. Variable $\rho(u, u_w)$ represents the hydrocarbon pore volume within the effective area. And the pore volume to a well $C\rho$ is defined as:

$$C\rho = \sum_{u \in \Omega} \rho(u, u_w) \tag{1.3.5}$$

For multiple well configuration, a total of the $C\rho_w$ is calculated, the hydrocarbon cumulative pore volume($CC\rho_w$)

$$CC\rho = \sum_{w=1}^{n_w} C\rho_w = \sum_{w=1}^{n_w} \sum_{u \in \Omega} \rho(u, u_w), \ n_w \text{ is number of wells} \tag{1.3.6}$$

$CC\rho$ represents the hydrocarbon that could be produced or drained by the wells. It is also suggested as a criteria for well planning. For a given number of wells, we

prefer the well configuration with the greatest $CC\rho$. This is similar to the criteria CCV stated above.

1.4 Optimization Considerations

1.4.1 Multiple Geostatistical Realizations

Each geostatistical realization is equally likely but would have different optimal configuration of wells. In practice, however, we need a single optimal configuration of wells that is "optimal" over all realizations simultaneously.

Applying the algorithm through multiple realizations by using the same objective function, we could get an 'optimal' well configuration. The "optimal" configuration may not be optimal for each individual realization, but is optimal in expected value over all realizations. This meets the requirement of reservoir management: to make decisions based on unavoidable uncertainty.

1.4.2 Interaction Between Wells

For multiple well configurations, There are interactions between wells for both static and dynamic criteria. Under static context, geo-objects being drained by one well cannot be counted in by another well. For pore volume, we have similar interactions with slight difference. For geo-objects, only geo-objects 'directly' perforated by well bore and the part within the drainage area is counted in as CCV connected to this well, but for pore volume, any pore volume within the drainage area could be counted in as PV.

1.5 Optimization Algorithm

Consider n_x, n_y, n_z to be the number of grid nodes along the x, y, z axes of a 3-D model, n_{Dip} to be the number of intervals for dip, $n_{Azimuth}$ to be the number of intervals for azimuth, and n_w to be the number of wells. Assuming every movement has equal chance, there will be $nx \times ny \times nz$ candidate locations for each well. Accounting for angle intervals, the number of possible candidate angles are $n_{Dip} \times n_{Azimuth}$. The possible configurations of n_w wells can be calculated:

$$N = \text{“}n_x \cdot n_y \cdot n_z \cdot n_{Dip} \cdot n_{Azimuth} \text{ choose } N_w\text{”} = \frac{n_x \cdot n_y \cdot n_z \cdot n_{Dip} \cdot n_{Azimuth}!}{(n_x \cdot n_y \cdot n_z \cdot n_{Dip} \cdot n_{Azimuth} - n_w)!} \tag{1.5.1}$$

For example, if we have a $100 \cdot 100 \cdot 10$ reservoir model,with 90 dip angle intervals and 360 azimuth angle intervals , and there are 5 well locations to be optimized, the number of possibilities may be calculated as:

$$1.62\times10^{19}\cdot(1.62\times10^{19}-1)\cdot(1.62\times10^{19}-2)\cdot(1.62\times10^{19}-3)\cdot(1.62\times10^{19}-4) = 1.12\times10^{46}$$

This is a huge number. It is simply not possible to consider.

Theoretically, the “true” optimal configuration could be found by searching the the entire configuration space. Although intractable for a large number of wells, we permit the user to consider the exhaustive search technique for one, two and three wells. Although the exhaustive algorithm can find the true optimal configuration, CPU requirements restrict its usage. A more efficient algorithm must be developed to solve the problem.

The well location optimization problem is a combinational maximization problem. The space over which the objective function (CCV or $CC\rho$) is defined is not simply

the N-dimensional space of parameters. Rather, it is a very large discrete configuration space, like the set of possible orders of cities in the famous traveling salesman problem. The elements in the configuration space is large, so that they cannot be explored exhaustively. Furthermore, since the well location set is discrete, any useful optimization notion, such as "continuing downhill in a favorable direction", is deprived of application in the well positioning problem. No such "direction" concept can be extracted and hence no direction to follow.

There are a number of candidate optimization algorithms that could be considered including genetic algorithms, simulated annealling[6, 22, 7, 23, 26], and a limited set of derivative-based methods. We consider an iterative scheme based on simulated annealing. For many applications, however, we do not need to perform a full simulated annealing with complex decision rule[19, 24].

Some features of this problem formulation:

1. Choose the number of wells to be optimized. The wells can be combinations of deviated wells and horizontal wells.

2. Initial configuration: select initial locations and well path categories. Well path categories are horizontal, deviated and vertical wells.

3. The initial objective function is evaluated as O_{ini}. The objective function is one of the following two functions:

   - Maximize connected volume CCV
   - Maximize hydrocarbon pore volume $CC\rho$

4. Perturbation Mechanism: randomly choose a well from the well pool and modify the well trajectory by randomly choosing the following options:

- Collar translate($move(\Delta x,\ \Delta y)$): defined as randomly select a distance for the well path $(\Delta x, \Delta y)$ within preset range and shift the whole well trajectory.
- Vertical move($upDown(\Delta h)$): defined as moving a whole well path with randomly selected height.
- Rotate($turnAround(\alpha)$): randomly choose an azimuth angle and rotate the well path around the starting point of the well bore.
- Tilt($tilt(\beta)$): tilt the well with randomly chosen angle. The angle could be restricted to a given range of dip. Deviated wells have defined all the four purtabations above, but vertical well overrides tilt and rotate to $move(\Delta x, \Delta y)$ and $upDown(\Delta h)$ individually. Horizontal well class then, overrides $tilt(\beta)$ with $turnAround(alpha)$.

5. Recalculate the objective function O_{try} for the new configuration
6. Decision rule: If $O_{try} > O_{pre}$, a better well configuration obtained. The current well configuration is accepted and O_{pre} is updated with current value O_{try}. If $O_{try} <= O_{pre}$, a well configuration is not as good as the previous one. The previous well configuration is retained and O_{pre} will keep the current value without updating. At this point, a "true" simulated annealing decision rule could be used.
7. The perturbation process step 4 is repeated a large number of times. In practice, the CCV reaches a maximum value and does not increase any more.

After this optimization procedure, we get CCV^*. If the cycles are enough and our starting point is good enough, we will get close to the "true" optimal configuration

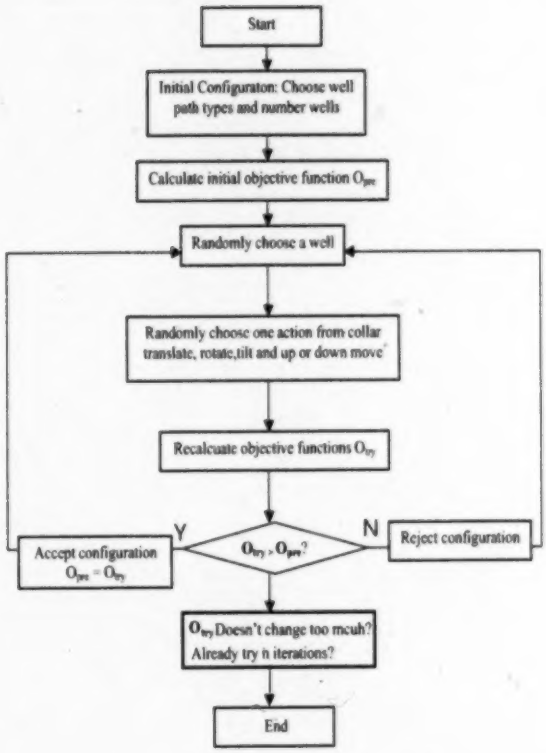
Start
Initial Configuraton: Choose well path types and number wells
Calculate initial objective function O_{pre}
Randomly choose a well
Randomly choose one action from collar translate, rotate,tilt and up or down move
Recalcuate objective functions O_{try}
Y
N
$O_{try} > O_{pre}$?
Accept configuration $O_{pre} = O_{try}$
Reject configuration
O_{try} Doesn't change too mcuh? Already try n iterations?
End

Figure 1.6: Flow chart for optimization algorithm

of well locations. In practice, we repeat the procedure with different random starting points to reduce the risk of finding a local maxima.

1.6 Flow Chart

A flow chart of the above methodology is given as in Figure 1.6.

1.7 Software Engineering

We have deviated , horizontal and vertical wells. A horizontal well "is-a" deviated well with dip equals 90 degree and azimuth of any arbitrary degrees; A vertical well "is-a" deviated well with dip equals 0 degree and no azimuth. In the view of Object Oriented Design(OOD)[12], "is-a" means inheritance, hence horizontal well inherits from deviated well and vertical well inherits from deviated well class. The Unified Modeling Language(UML) representation of the inheritance of these well types are shown in Figure 1.7. CDevWell is the base class for CVertWell and CHorzWell. CVertWell and CHorzWell are brothers or sisters. Please note the overriding behaviour of the three classes. The implementing language is Java[16, 17].

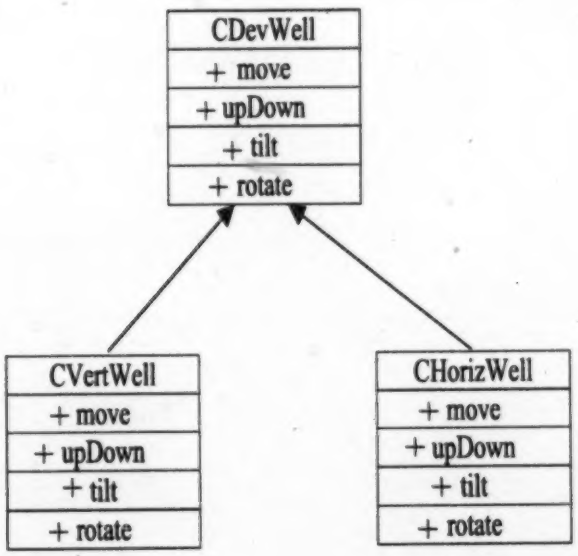

Figure 1.7: UML of well type classes

A deviated well can move areally, move up or down, tilt and rotate. We define the basic movements *move*, *upDown*, *tilt* and *rotate* as a well's four movement types.

- *move*(*double* Δx, *double* Δy): area movement of the whole well trajectory with distance $(\Delta x, \Delta y)$;
- *upDown*(*double* Δh): vertical movement of the whole well trajectory δh;
- *tilt*(*double* α): tilt well trajectory around well trajectory starting point with α where after tilting, the dip is within $(0, 90)$;
- *turnAround*(*double* β): rotate well trajectory around starting point with an angle β.

As for a horizontal well, it can not be tilted. In OOD, the '*tilt*' can be easily overridden to call super class's , that is *super.move*. In reality for a horizontal well planning, azimuth optimizing could have more priority, overriding *tilt* to *move* is reasonable. Here is implementation of *tilt* method in class $CHorzWell$:

```
public void tilt(double angle)
{
super.turnAround(double angle);
}
```

Vertical well doesn't have an azimuth, it shouldn't be tilted or rotated. We override *turnAround*(*double*) as follows, which gives more priority to height refining:

```
public void turnAround(double angle)
{
```

super.upDown(double angle);

}

This is the design and implementation of three well type classes. Now, the optimization class: all the implementation about optimization resides in *CWPOptimal* class. Optimization class "has a" deviated wells *CDevWell* to be optimized, which are the base classes of vertical well class *CVertWell* and horizontal well class *CHorzWell*. The main methods are *stir*(), *optimizeAllPurpose*(). The method *stir* is where perturbation techniques resides. It randomly chooses a well in pool, randomly choosing a type of movement with randomly chosen distance or angle.

The method *optimizeAllPurpose* is the core method which follows working flow as shown in Figure 1.6. It has an integer option called *optimize2What* which is used to specify refining priorities as listed below:

- 0 = location(1/3 chances), dip(1/3 chances), azimuth(1/3 chances);
- 1 = all but 1/2 chances on well location;
- 2 = dip(100 percent);
- 3 = dip(50 percent), azimuth(50 percent);
- 4 = location(100 percent) only.

Client program then calls with the appropriate option according to user's demands. For example, a well is put to somewhere and we prefer the position. What we are not sure is the directional parameters of this well. The option 3 listed above is chosen to refine the azimuth and dip. For a well with no preference of location, option 0 is used to refine every aspect of a well.

This is the reason why the algorithm could be used sequentially which is highly recommended by the author. This gives more chance to refine target parameters and hence better results will be expected.

There are, however, other supporting classes, such as $CLocationIn$, $CTargetIn$, which are used to find reservoir cells within the drainage radius. $CTargetIrregularIn$ is used to define a irregular drainage area. In the case when a fault is encountered, we could define the drainage area constrained by faults. The code of handling irregular drainage area is complete and in the package, but I have not got a chance to test it.

Chapter 2

Testing and Validation

2.1 Homogeneous Model

One way to check how wells are positioned is to consider a "homogeneous" 3D model. Here we generate a $100 \cdot 100 \cdot 1$ model with every node in the model being geo-object 1. Given constant porosity, the volume of each node is identical. We test the algorithm on this model with different number of wells.

Suppose there are 16 wells with radius 10(cells) to be optimized. Since the overall reservoir is $100 \cdot 100$ nodes, there is more space than the sum of the drainage areas. Hence, we expect the optimal well configurations distributed without overlapping. Figure 2.1 shows how the optimization algorithm distributes the 16 wells. There is no overlap. The objective function CCV is maximum.

Trying to increase radius to 17 but cut down well number to nine leads to even distribution of wells; however, the optimal configuration would minimize such overlap. Drainage area(circles) of these 9 wells are expected to be nearly tangent as shown in Figure 2.2. The 9 well locations do not overlap much.

Figure 2.3 shows the results if further increasing the drainage radius to 20 for the

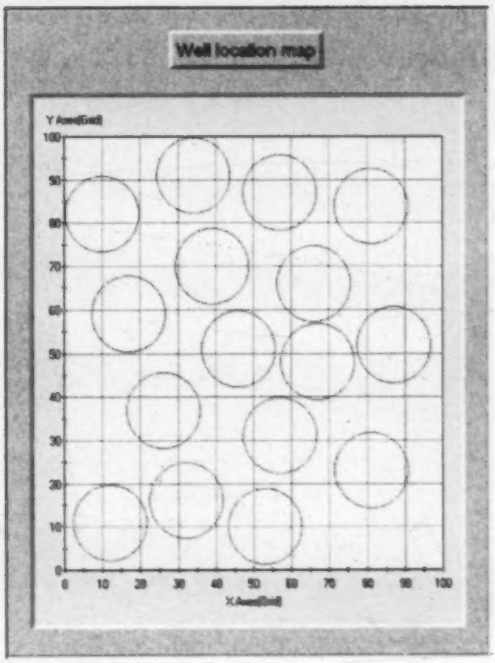

Figure 2.1: Well locations of 16 wells with radius 10. The wells are evenly distributed without overlapping each other.

example above. The wells overlap by a nearly constant amount. The configuration shown on this figure reflects what we are expecting. Figure 2.4 shows the CCV versus iteration through the optimization process.

Consider 10 wells with radius of 20. These 16 wells are to be optimized. The total drainage area is bigger than the whole reservoir area. So, the optimized configuration should cover the entire reservoir. In this case, there is a total CCV of 10,000(units) available to be drained. Figure 2.5 shows the initial well configuration half way through the optimization process, and the final well configuration. What we can see is how the well configuration moves from randomly distributed to evenly distributed. The drainage area of these 16 wells totally covers the reservoir field. At the end of

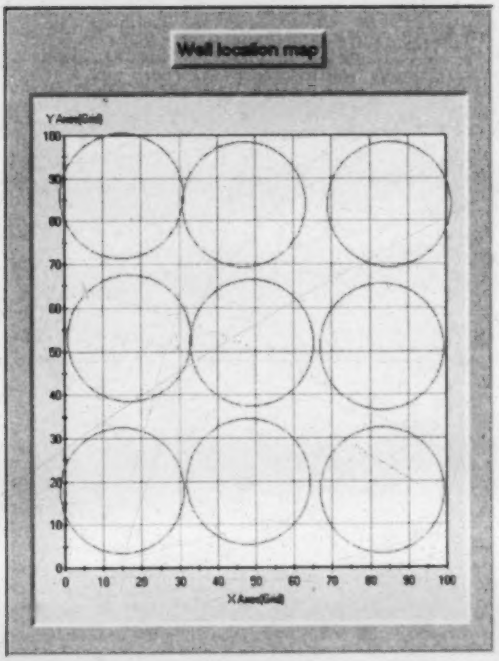

Figure 2.2: Well location map of 9 wells with drainage radius 17. These 9 wells are nearly tangent.

optimization, the algorithm has found the maximal CCV of 10,000. Once this non-overlap configuration is obtained, there will be no improvement of CCV then the configuration was frozen until the iteration ends.

2.2 Heterogeneous Model

We use *Sisim* (GSLIB)[15, 8] to generate a 50*50*1 heterogeneous model. The reason for a 'simple 2D model' is that it is easy to judge the results of the well locations and CCV map without complex calculation. Figure 2.6 shows the image map of the model. The black color represents the geo-object 1 and other gray scale colors represent other geo-objects with the color change respectively (from 2 to 16).

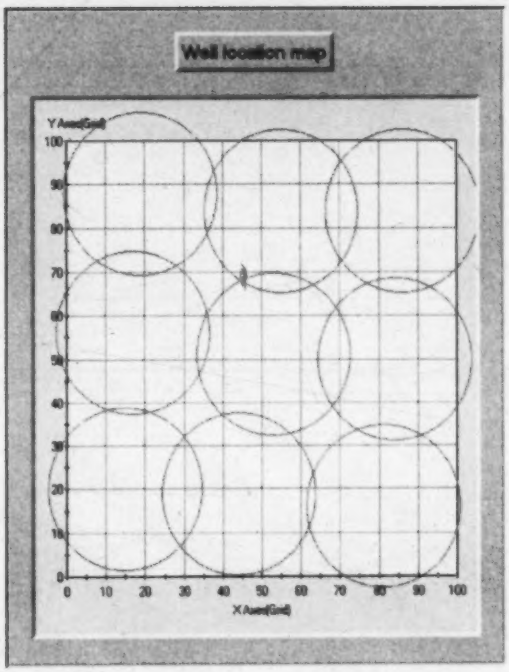

Figure 2.3: Well location map of 9 wells with radius 20. These 9 wells distributed evenly with 3 columns by 3 lines.

Convergence

The stochastic optimization algorithm may be sensitive to the initial configuration. Figure 2.7 shows three different initial configurations and the optimal configurations. Although the program starts with different initial well locations, the algorithm finds nearly the same optimal configuration in all cases.

Our experience is that the optimal solution does not vary significantly with different initial realizations. Nevertheless, we advise users to consider a number of initial configurations. Also, to some extent (particularly for 2-D models) the final result can be checked visually.

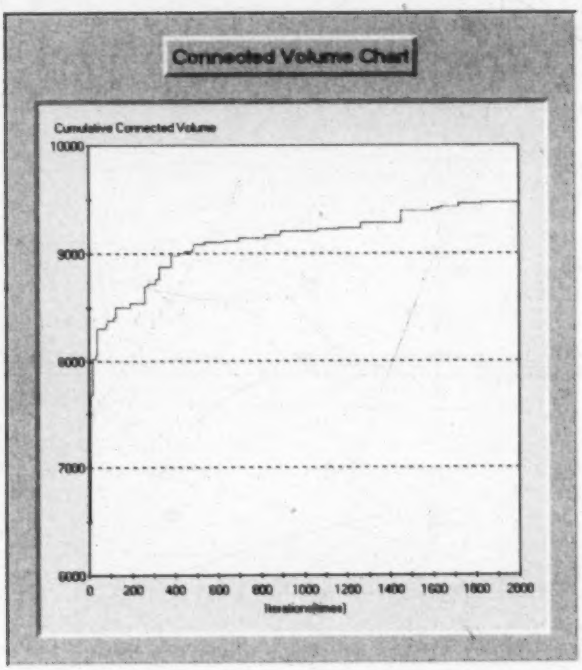

Figure 2.4: The CCV chart of 9 wells with radius 20.

Comparison with True Result

CPU time consumption is tested on the realistic example. For one well of radius 10 configuration, the CPU time need for enumerate algorithm is 5 seconds and the time needed for optimal is 5.5 seconds(see Figure 2.8). In this case, we cannot find the strength of our optimization algorithm.

But, when we start to test 2 wells of radius 10, the CPU time needed for these two algorithms are quite different! The enumerate algorithm needs 10.5 hours while the optimization one needs only 15.5 seconds on a Pentium II 333MHz computer with 128 MB RAM. Figure 2.9 shows the end well location maps. The exhaustive algorithm gets 6 out of 365 units of CCV more than optimization algorithm.

We estimate that the time needed for a 3 wells of radius 10 case should be 250,000

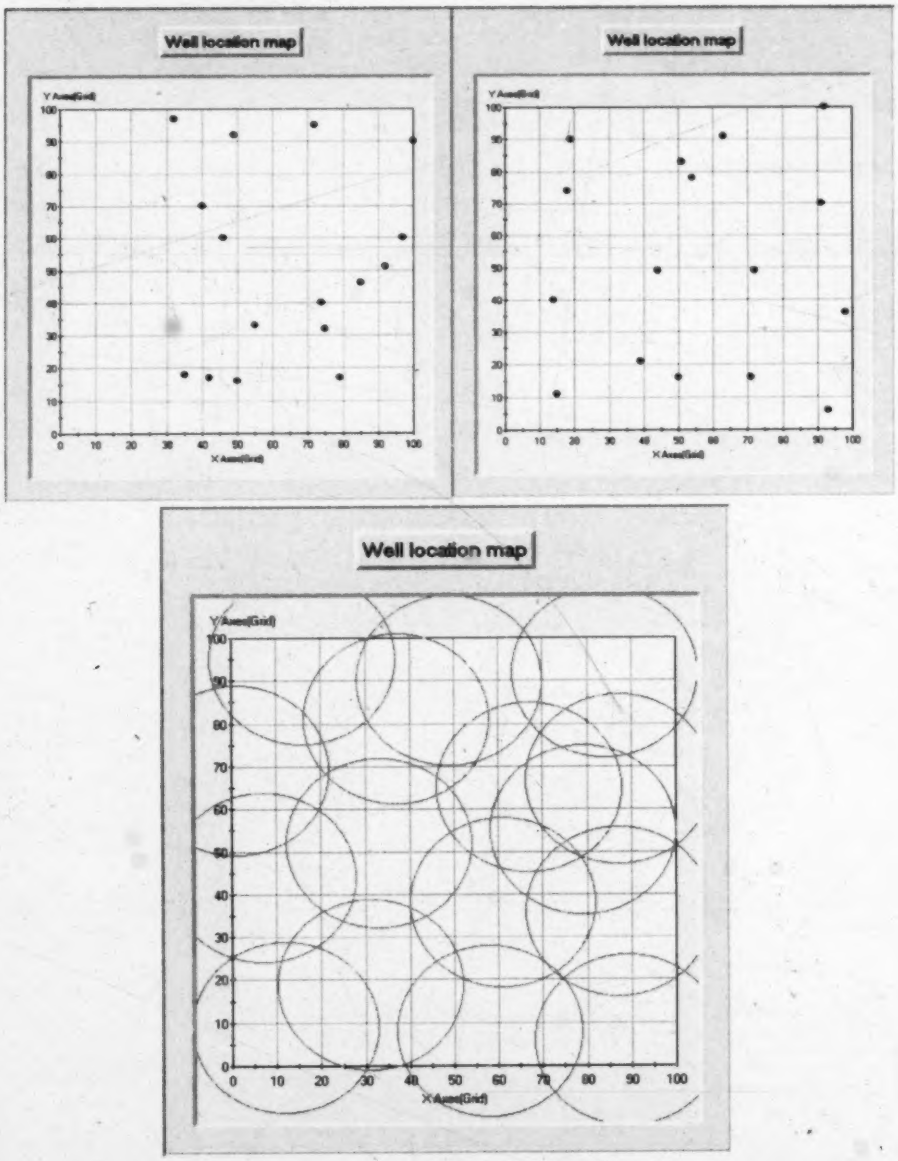

Figure 2.5: Distribution and overlapping for 16 wells with radius 20.

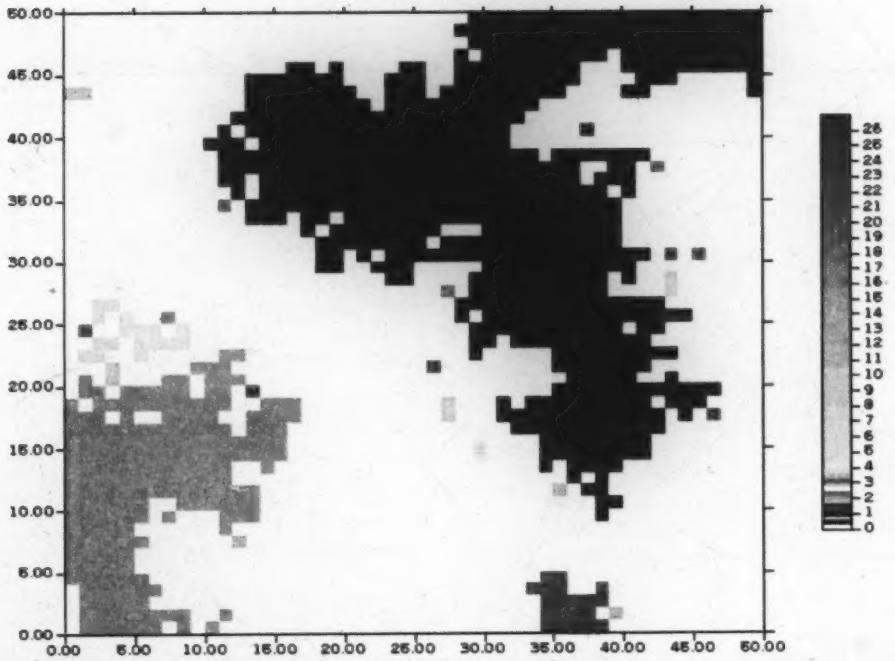

Figure 2.6: The image map of simple model (50*50*1). The black color represents geo-object 1. There are 26 geo-objects of this model. The gray colors represent the corresponding geo-objects.

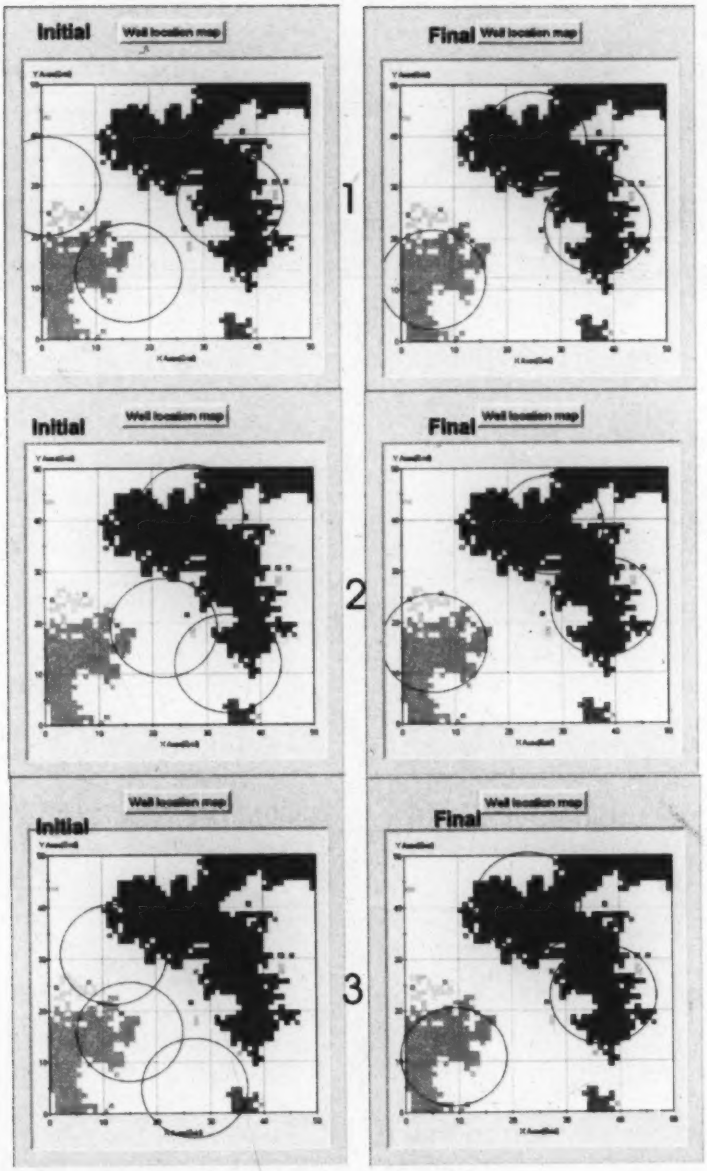

Figure 2.7: Three different initial and final realizations. Note that the same result is obtained in all cases.

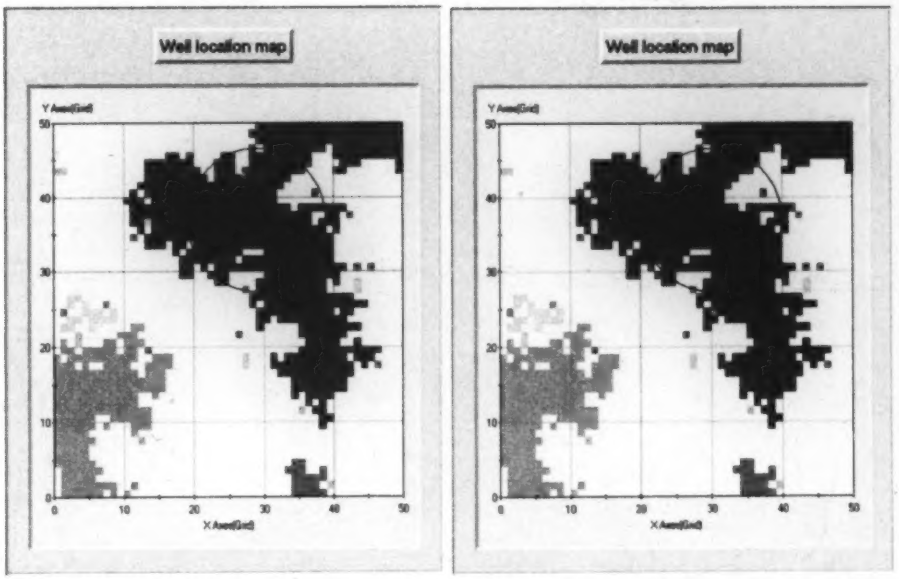

Figure 2.8: Result of optimal algorithm and result of exhaustive search for one well.

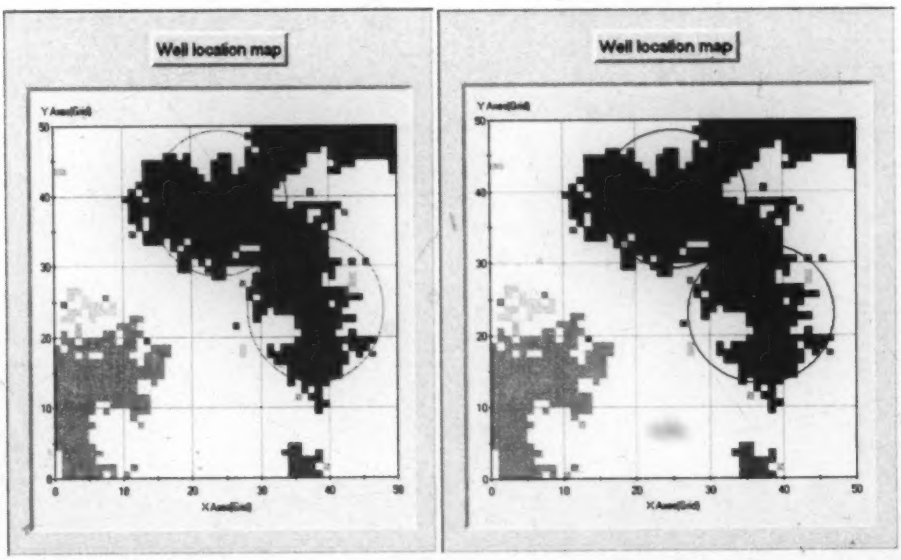

Figure 2.9: Result of optimal algorithm and result of exhaustive search for two wells.

hours of CPU time! For reference, the time need of this case for optimization algorithm is only 37 seconds.

2.3 3-D Heterogeneous Model

Figure 2.10 shows different views of a $100 \cdot 100 \cdot 10$ reservoir model. This is based on a real reservoir (Gouveia et. al. 1997) but shown with no scale or structural component. The different colors represent facies of different reservoir quality. There are six different geo-objects, that is, six different flow units. Although this model is more complex than the other 3-D models considered here, the program works the same.

Figure 2.11 show the optimal well locations for 1 and three wells. Any combination of wells with different drainage radii could be considered.

2.4 Exhaustive Example

Sequential indicator simulation (`sisim` in GSLIB) was used to generate a 100 by 100 2-D model to test the optimization algorithm. Figure 2.13 shows the geo-objects resulting from an unconditional `sisim` model. Results for using an increasing number of wells is shown on Figures 2.14, 2.15, 2.16, and 2.17.

At times it is necessary to decide on the optimal number of wells to produce a field. The production rate and details of well productivity can be established by classical petroleum engineering calculations. The analysis we present here, however, could be used to ascertain the additional reservoir volume that could be drained by using more wells. A plot of the optimal CCV versus the number of wells could be created. The

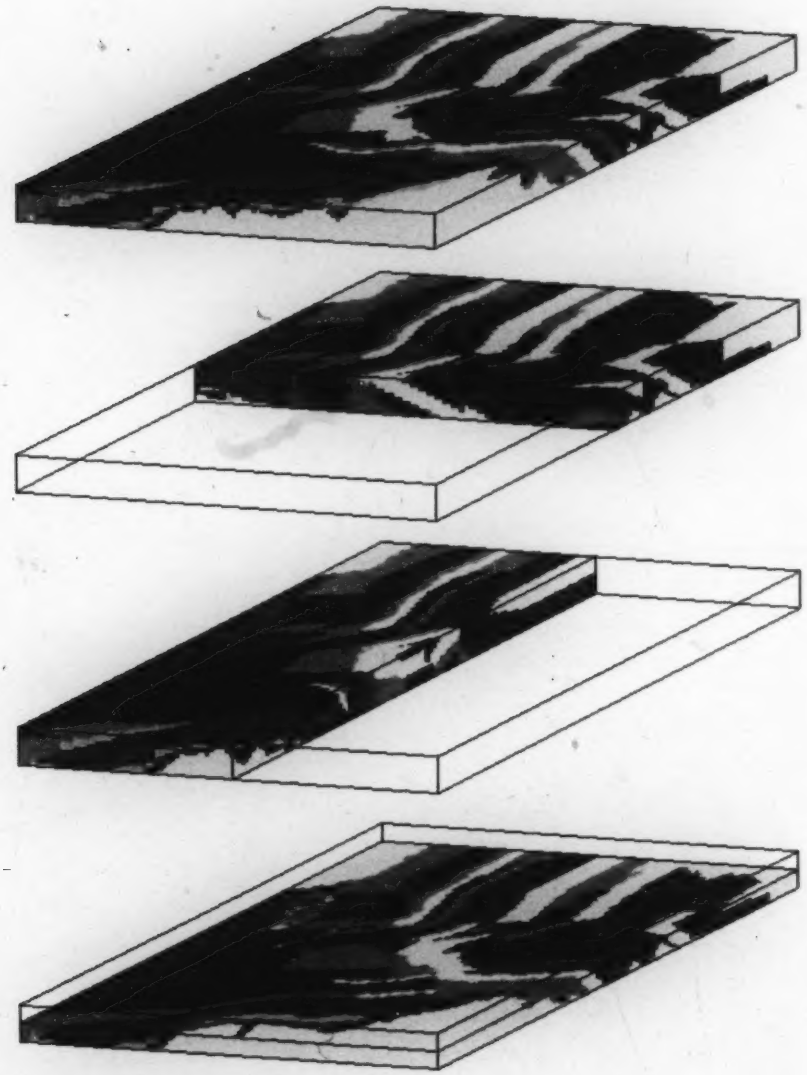

Figure 2.10: Different views of a real 3-D reservoir model.

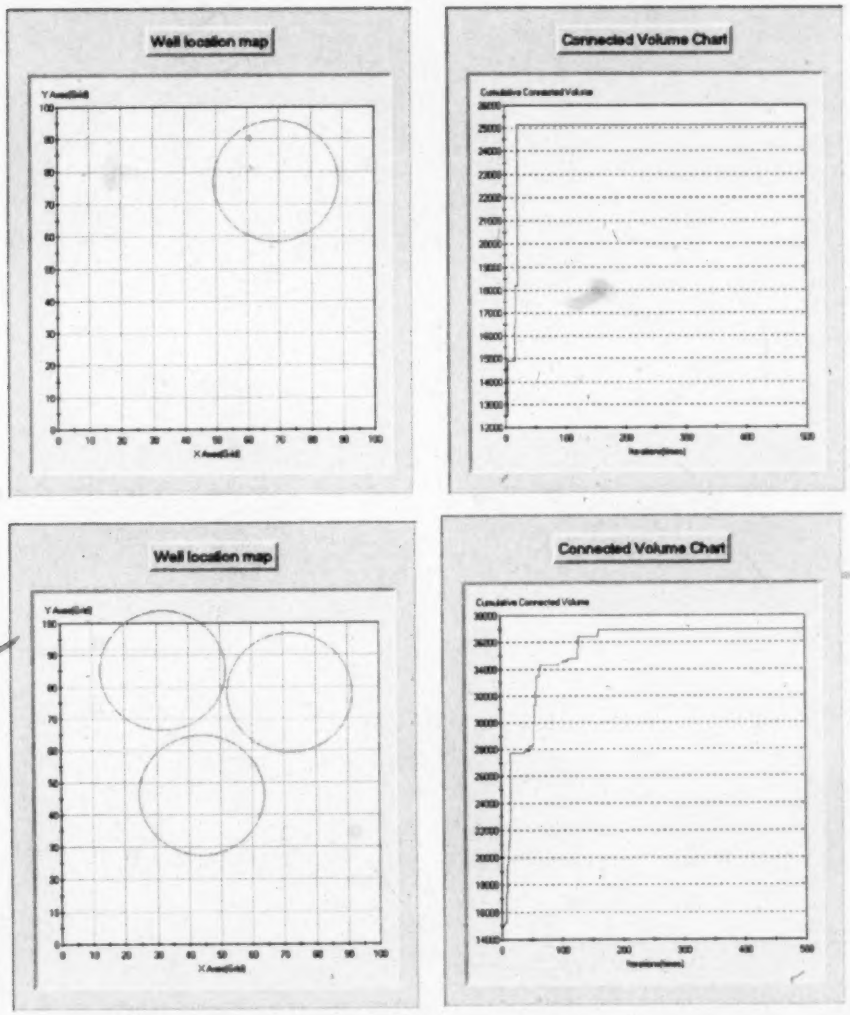

Figure 2.11: results of 1 and 3 wells for 3-D reservoir model.

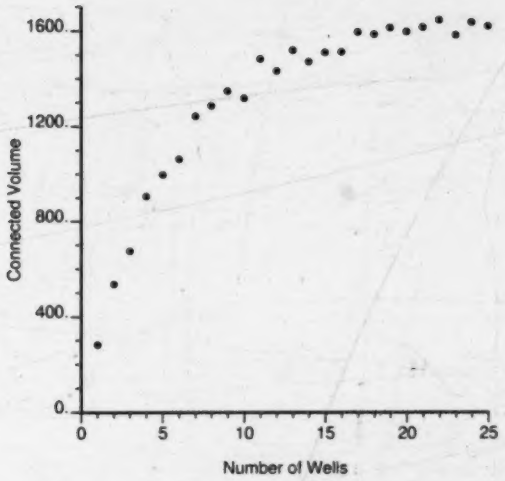

Figure 2.12: Cumulative recovery for different numbers of wells. Note that the non-monotonic behavior is due to some randomness introduced by different initial realizations.

incremental recovery with additional wells can be considered to determine the point where the cost of a well is not justified by the incremental recovery. Figure 2.12 shows the relationship of cumulative recovery versus the number of wells.

2.5 Multiple Realizations

With Sisim (GSLIB), we can also generate multiple realizations. Each realization is equally likely and would have a different optimal configuration of well locations. In practice, however, we need a single optimal configuration of wells that is "optimal" over all realizations simultaneously. As presented in the methodology section, this can be used in the objective function.

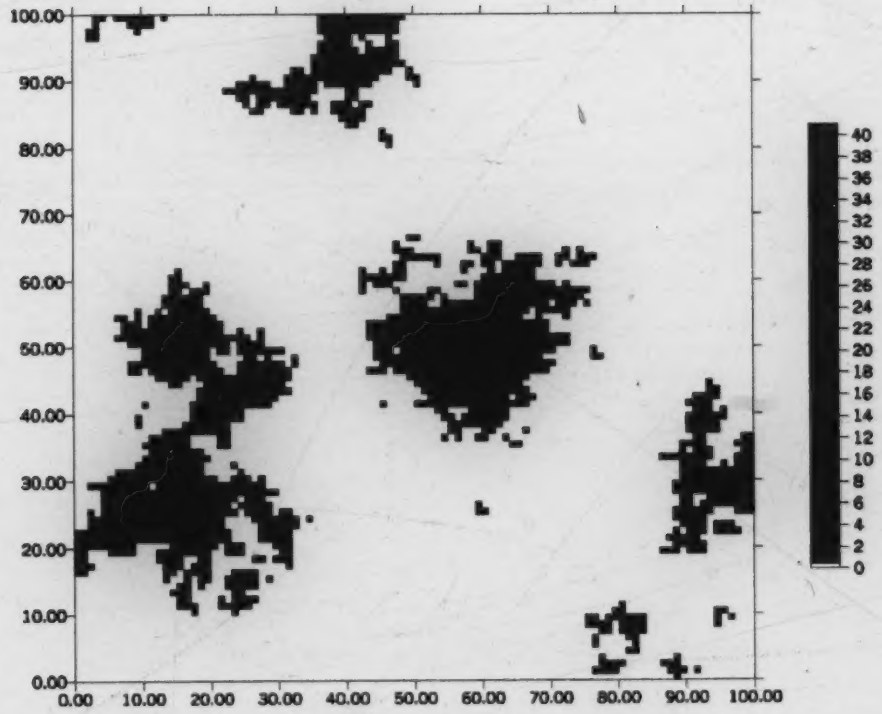

Figure 2.13: Geo-objects in exhaustive example.

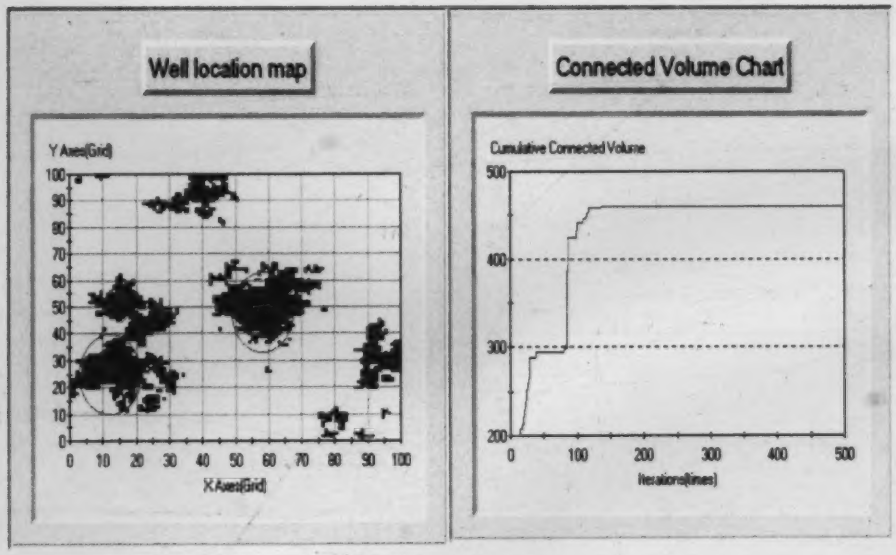

Figure 2.14: Results of 2-wells of radius 10.

Four 2-D realizations with dimension $50 \cdot 50$ were generated by `sisim`, see Figure 2.18. The geo-objects are calculated for each image and the optimal well configurations (for 1, 2, and 3 wells) are then obtained. These globally optimal configurations are not optimal for each realization, but *in expected value* over all realizations. This is precisely the goal of reservoir management, that is, to make decisions that are robust with respect to the unavoidable uncertainty. Table 2.1 shows the CCV for the four different realizations. These results quantify the uncertainty in the reservoir response for this particular decision.

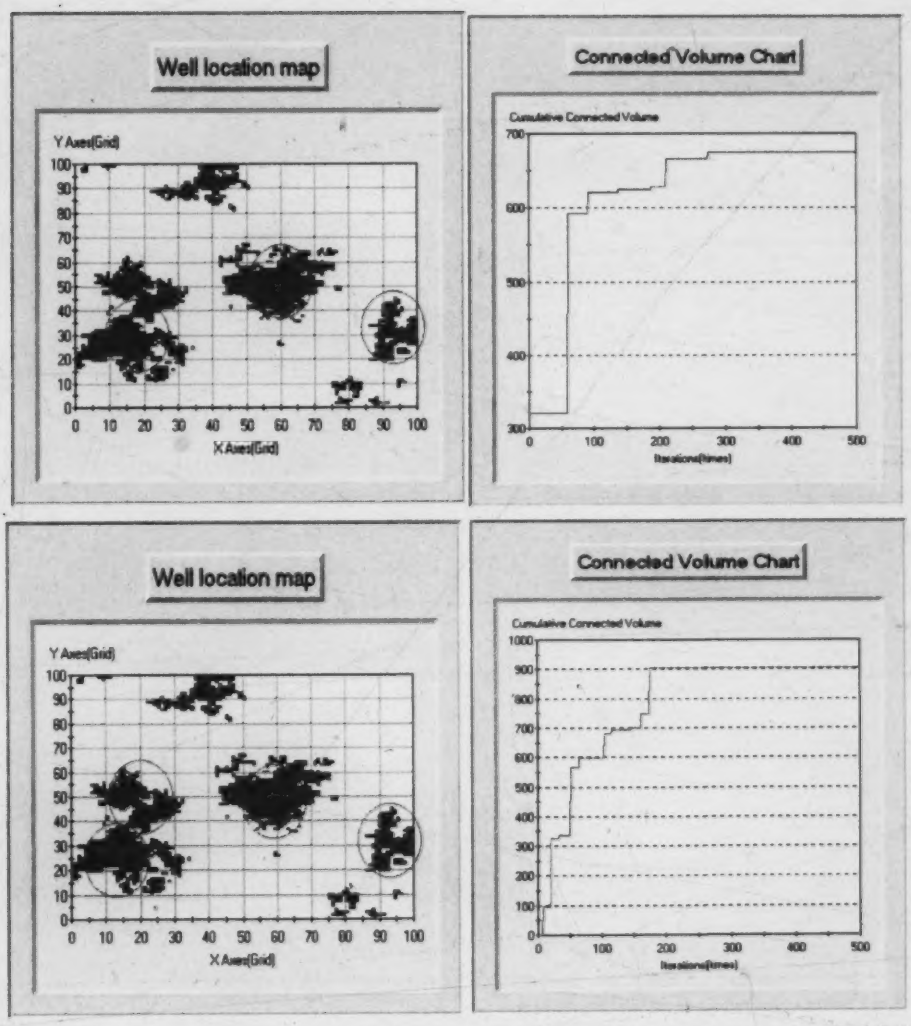

Figure 2.15: Results of 3 and 4 wells of radius 10.

Realization Number	CCV
1	1932
2	2935
3	2794
4	2881

Table 2.1: CCV of each realization.

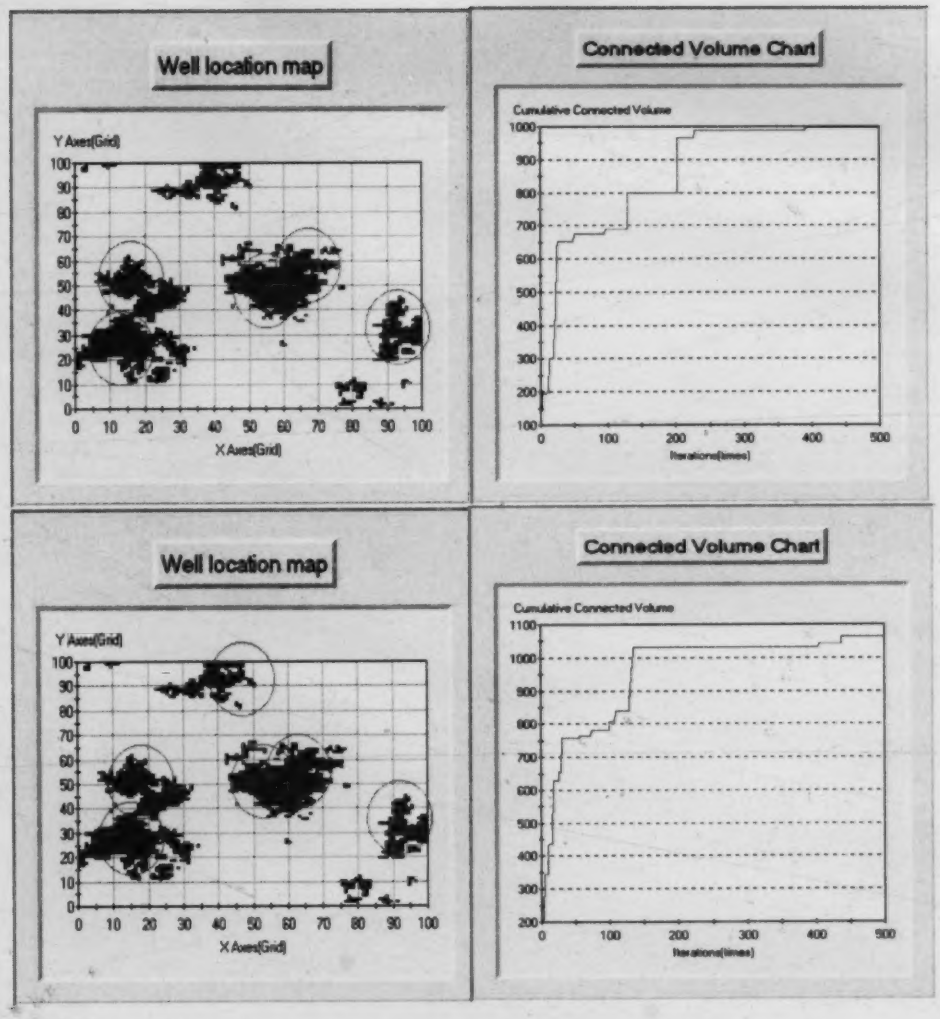

Figure 2.16: Results of 5 and 6 wells of radius 10.

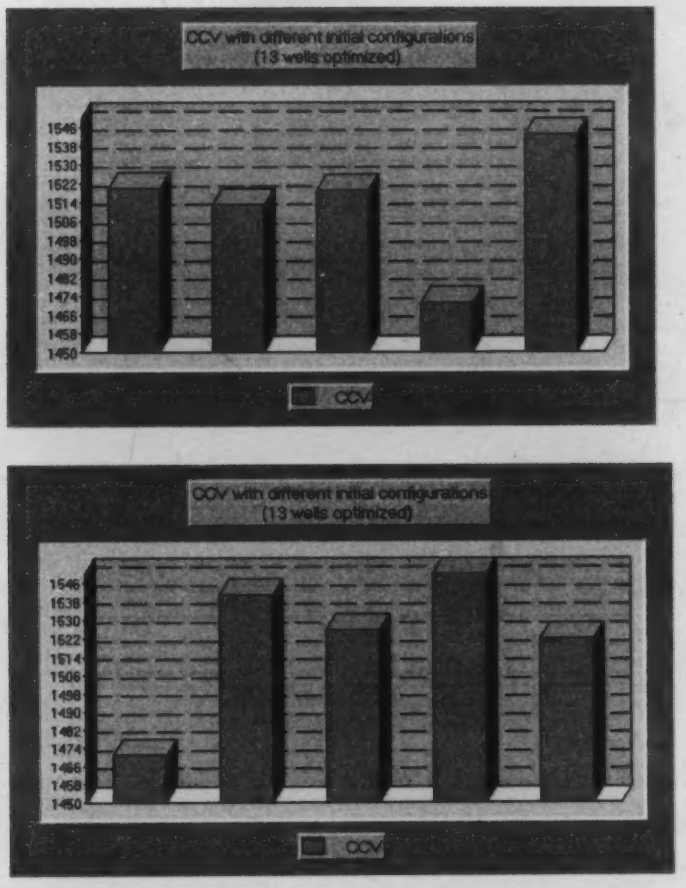

Figure 2.17: Multiple results with different initial configurations for 13 wells and 14 wells. Note the greater maximum value for the 14 well case.

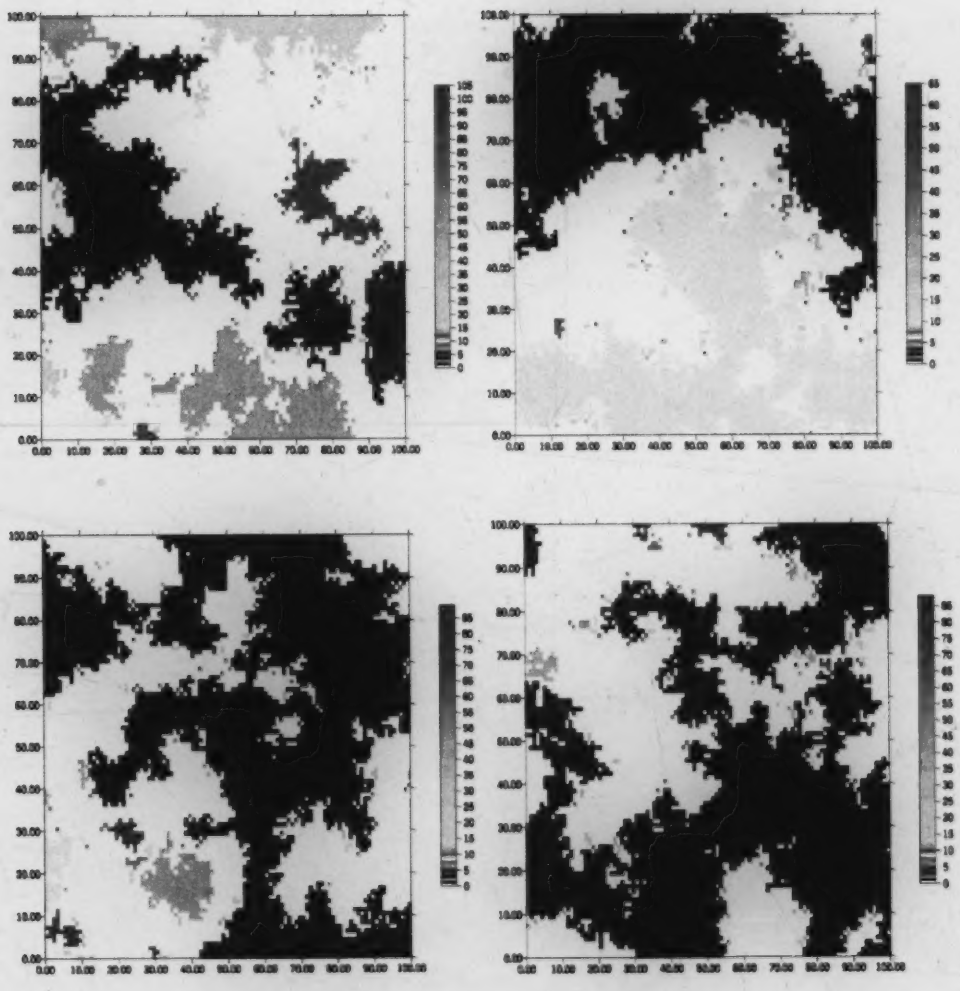

Figure 2.18: Four realizations for multiple realization example.

2.6 A Real Example With Multiple Well Types

Since this algorithm is implemented in Landmark Graphics Co. development environment, it takes advantage of industry leading technologies, such as GOCAD topology, 3D visualization etc. We are able to present some of the testing results for the algorithm.

The reservoir has $91 \times 71 \times 28$ grid nodes represented by GOCAD SGrid data format. User can visually pick a initial well position and edit parameters, such as dip, azimuth, drainage radius and drainage shape. This is the "initial configuration". In the well planning menu, we add one menu item called "optimize" to call the algorithm. By checking the check box besides the well, user specifies which wells to be enrolled in optimization. Number of iterations must also be specified.

After optimizing, the visualization tool brings the resulting well configuration and original configuration to the user. We could easily check well locations, dip, azimuth, drainage area, interactions and objective functions.

Figures 2.19, shows how one deviated well optimized in two continuous layers. The original and optimized well have been marked. By comparing the performance and objective function values of the individual cells, we found that the objective function is much higher than the original configuration, which means that a better well configuration has been found.

A preexisting well can affect optimization. But, by un-checking the including box in the optimize dialog, a well can be exempted from the optimization, which means discount the effect of the well.

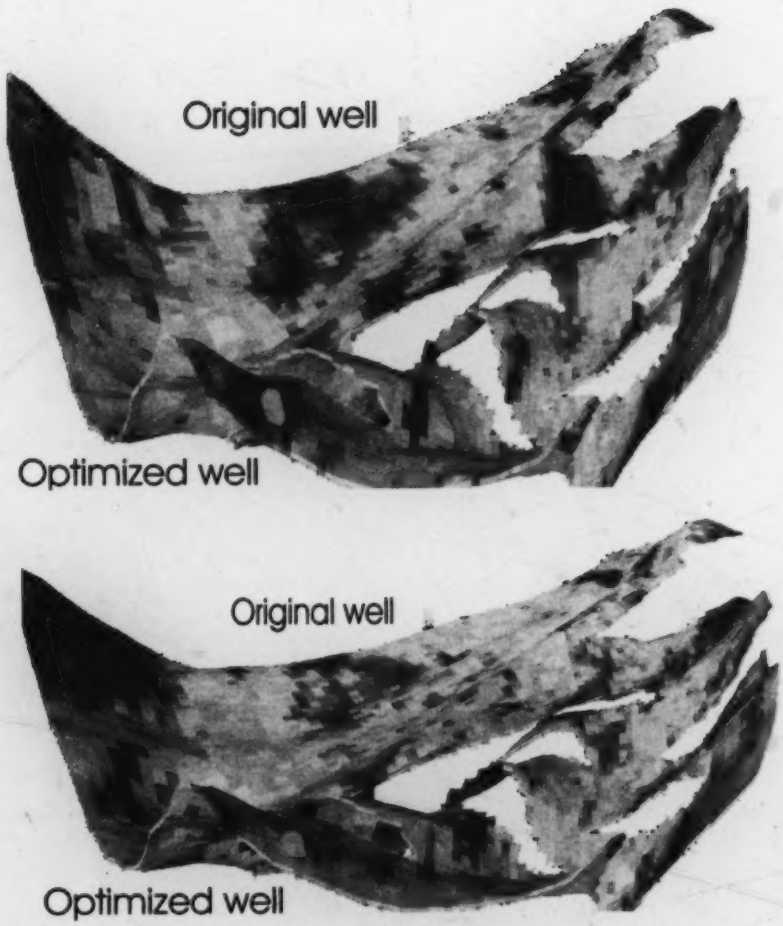

Figure 2.19: Optimizing one deviated well, in two consecutive layer. Cylinder shape of the well represents the drainage radius.

Chapter 3

Limitations and Future Work

3.1 Additional Constraints

3.1.1 Productivity

Permeability k is an important parameter of reservoir, which calibrates a reservoir's productivity. Permeability k is related to how easy fluids can be produced. In well planning, we prefer the well configurations with higher quality reservoir to be closer to the well bore. That is to say, exclusive of permeability itself, distance affects the end results. Permeability as a component objective function can be defined as follows:

$$O_k = [\sum_{i=1}^{n_{cell}} \frac{1}{d_i} \cdot k_i^{\omega}]^{\frac{1}{\omega}} \tag{3.1.1}$$

where d_i represents the distance from the cell to well bore, n_{cells} represents the cells inside the drainage area. Power law average technique is employed due to the nonlinearity of permeability.

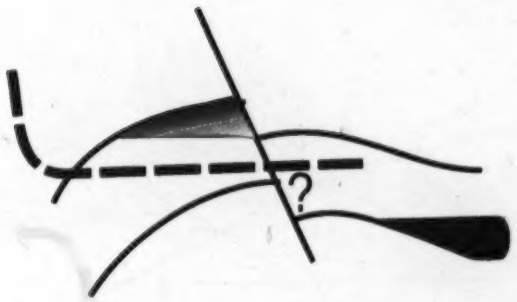

Figure 3.1: Schematic illustration showing that considering faults as restriction.

3.1.2 More Complex Geological Structure

Geologic structure influences oil and gas accumulation and drainage in many ways and should be taken into account in planning wells.

One important geological phenomenon is faults. Faults are important for well planning. One restriction could be to avoid well trajectory from crossing the fault, refer Figure 3.1.

3.1.3 Fluid Contacts

The closeness of the well to the oil water contact may be defined as a penalty by

$$O_{wc} = m_1 - l_{wc} \tag{3.1.2}$$

where,

$$l_{wc} = \sqrt{(x_w - x_c)^2 + (y_w - y_c)^2 + (z_w - z_c)^2} \tag{3.1.3}$$

w is the closest point on the well path to the fluid contact plane., c is the fluid contact plane, and m_1 is a constant associated with distance from well trajectory to

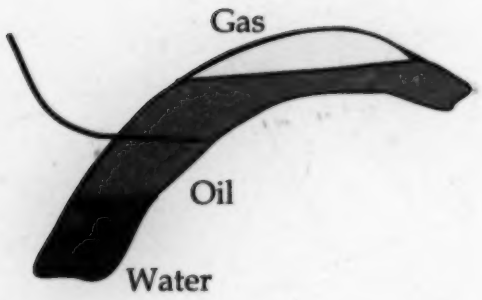

Figure 3.2: Schematic illustration showing multi-fluid contacts.

fluid contact. Gas oil contact restriction could be defined similarly. Figure 3.2 depicts the idea of where a well trajectory should put between multi-fluid contacts.

3.1.4 Tortuosity

Tortuosity constraint can be evaluated as the average tortuosity factor of all the geo-object(s) perforated. Due to the drainage radii restriction, only the geo-objects within the radii are included.

$$O_{tor} = \frac{1}{n_w}\frac{1}{n_g}\sum_{w=1}^{n_w}\sum_{g=1}^{n_g} t_{geo_i} \tag{3.1.4}$$

Where, n_w is number of wells in the reservoir and n_g is number of geo-objects each well perforates. The less tortuosity, the less penalty.

In Figure 3.3 both regions at right have same volume, but lower one is better. Measure of surface area to volume ratio is used to represent tortuosity. Figure 3.3

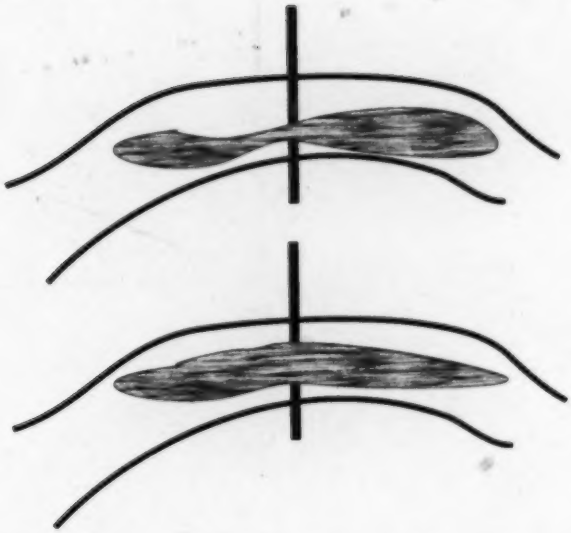

Figure 3.3: A well is likely not to be placed where more tortuous spot.

shows two geo-objects with same CV, but apparently, the lower schematic is better. Since, upper scheme is more tortuous than lower one.

3.1.5 Drilling Constraints

In real drilling practice, there are some constraints on well locations. For example, when a well is drilled offshore, the platform is fixed. The well starting points are close the platform and must be practical to drill from the platform. More restrictions on well interaction is required in such cases.

3.2 Combining Component Objective Functions

With more and more objective functions being introduced into the evaluations, a weighting technique that can combine them together into one overall function is demanded. Generally speaking, we could define the objective function as follows:

$$O_{all} = \sum_{i=1}^{n} \omega_i O_i \tag{3.2.1}$$

where ω_i and O_i are the weights and component objective functions, respectively. The component objective functions represent different constraints from geology, engineering and economic stated above. What we have discussed so far are CCV, $CC\rho$, permeability, porosity, tortuosity, geologic structures etc.

These constraint objective functions O_i $i = 1, ..., n$ could be expressed in widely different units of measurement. For example, a CCV measures the connected volume in cubic feet, while tortuosity O_{tor} measures the tortuosity for geo-objects which is a factor in (0,1). Weighting components equally causes the component with the largest magnitude dominating the global objective function, while the smallest magnitude will be, comparatively, omitted.

The weights ω_i is introduced to account for the contributions of each component with respect to its importance in the global objective function O_{all}. According to the algorithm, the global objective function O_{all} is used to determine whether to accept or reject a perturbation.

$$\Delta O_{all} = \sum_{i=1}^{n} \omega_i (O_{inew} - O_{iold}) = \sum_{i=1}^{n} \omega_i |\Delta O_i| \tag{3.2.2}$$

An easy rule of thumb tested by Deutsch [6] is that, making each component

contributes equally to the change in the objective function ΔO_{all}. Thus, each weight is determined by inversely proportioning to its absolute value:

$$\omega_i = \frac{1}{\Delta O_i}, i = 1, ..., n \tag{3.2.3}$$

Since, in practice, the average change defined above couldn't be determined before hand. Some kind of evaluation with given number N(say 500) of independent perturbations must be run and to obtain the average change $\overline{\Delta O_i}$:

$$\overline{\Delta O_i} = \frac{1}{N} \sum_{i=1}^{N} |(O_c^{(n)} - O_i)|, i = 1, ..., N \tag{3.2.4}$$

where $O_i^{(n)}$ is the perturbed objective value, and O_c is the initial objective value. The global objective function then is written to be:

$$O_{all} = \frac{1}{O^{(0)}} \sum_{i=1}^{n} \omega_i O_i \tag{3.2.5}$$

Where $O^{(0)}$ is its initial value which normalizes the objective function.

There are also other considerations, such as whether the relative importance of each component. Un-equal weighting techniques could be applied to the circumstances when the global objective function O_{all} cannot be lowered to zero.

3.3 Optimization Algorithm

3.3.1 Local Minima

There is a movement setting in both x and y directions. They control how far a well can move to. Given a dx and dy are chosen randomly by the algorithm, then the

distance of this well will move simply is:

$$d = \sqrt{dx^2 + dy^2} \tag{3.3.1}$$

If within d distance away from the well, there is no 'good' configurations accepted. Then the optimization is only within this area, which is defined as centering at this well location with radius d defined above. Simulated annealling solves this problem by accepting randomly 'bad' configurations, here 'bad configurations' are configurations which produce worse results of objective function. With some 'bad configurations' as its bridge, it will jump out of the 'local minima'.

3.3.2 Number of Iterations

For a 3D reservoir, there are millions of cells. The candidate configurations for multiple wells are tremendous. In addition, many iterations are needed to refine dip and azimuth.

For the number of iterations, a percentage relatively to the total candidates well configuration is unable to provide. Since for the example with $100 \cdot 100 \cdot 10$ reservoir model,with 90 dip angle intervals and 360 azimuth angle intervals , and there are 5 well locations to be optimized, the number of possibilities is 1.12×10^{46}. Even for a 0.001 percent of that would be 1.12×10^{43}. It is still not realistic for current CPUs. Maybe a true simulated annealing could be considered.

A sequential optimization process could also be considered to lower down the number of iteration, and the CPU time. Instead of trying to optimize location, dip, azimuth altogether, these steps could be done separately. In real world, the most crucial is to determine the location and then dip and azimuth. The first step is to optimize location only. All the iterations are given to refine the well locations

optimization. After this, an 'optimal well configuration' is obtained. Now, dip and azimuth of these wells need to be optimized. In the algorithm, we set all the iterations to refine dip and azimuth.

3.4 Summary and Conclusions

As described in our examples, this algorithm is directly applied to find the optimal well locations, such as production well sites. The algorithm provides input to reservoir simulation. Before costly and time consuming reservoir simulation, it provides suitable configurations. The CCV as well as $CC\rho$ statistics could also be used to rank multiple geostatistical realizations for uncertainty assessment with full reservoir simulation.

There is a need to rigorously account for the predictions of flow simulation in reservoir decision making. The work presented here uses "static" connectivity measures as a proxy for the full "dynamic" response of the reservoir. The optimization algorithm is intended to complement conventional flow simulation and geological input to well location selection.

The efficiency and speed of the optimization algorithm provides a tool to optimize drilling plans and development schemes, which permits improved economics and reduced risk.

Bibliography

[1] A. Cheng. Gocad in a hurry. Unpublished manual: Created and modified for ASGA Nancy, France, 1997.

[2] T. C. Coburn. Reflections on the profiferation of geostatistics in petroleum exploration and production. In J. M. Yarus and R. L. Chambers, editors, *Stochastic Modeling and Geostatistics: Principles, Methods, and Case Studies*, pages 21–23. AAPG Computer Applications in Geology, No. 3, 1995.

[3] P. S. da Cruz and C. V. Deutsch. Reservoir management decision making in presence of uncertainty. Centre for Computational Geostatistics Report Two:1999/2000, 2000.

[4] C. V. Deutsch. Relative influence on flow performance of spatial heterogeneities versus uncertainty in relative permeability curves. In *Report 3, Stanford Center for Reservoir Forecasting*, Stanford, CA, May 1990.

[5] C. V. Deutsch. Fortran programs for calculating connectivity of 3-d numerical models and for ranking multiple realizations. *Accepted for Publication in Computers & Geosciences*, 1998.

[6] C. V. Deutsch and P. W. Cockerham. Practical considerations in the application of simulated annealing to stochastic simulation. *Mathematical Geology*, 26(1):67–82, 1994.

[7] C. V. Deutsch and A. G. Journel. The application of simulated annealing to stochastic reservoir modeling. In *Report 4, Stanford Center for Reservoir Forecasting*, Stanford, CA, May 1991.

[8] C. V. Deutsch and A. G. Journel. *GSLIB: Geostatistical Software Library and User's Guide*. Oxford University Press, New York, 2nd edition, 1998.

[9] C. V. Deutsch and S. Srinivasan. Improved reservoir management through ranking stochastic reservoir models. In *SPE/DOE Tenth Symposium on Improved Oil Recovery, Tulsa, OK*, pages 105–113, Washington, DC, April 1996. Society of Petroleum Engineers. SPE paper number 35411.

[10] C. V. Deutsch and T. T. Tran. Fluvsim: A program for object-based stochastic modeling of fluvial depositional systems. *Submitted to Computers & Geosciences*, 1998.

[11] C. V. Deutsch and L. Wang. Hierarchical object-based stochastic modeling of fluvial reservoirs. *Math Geology*, 28(7):857–880, 1996.

[12] M. Fowler, K. Scott, and G. Booch. *UML Distilled, Second Edition: A Brief Guide to the Standard Object Modeling Language*. Addison-Wesley Pub Co, 1999.

[13] D. J. Goggin, J. Gidman, and S. E. Ross. Optimizing horizontal well locations using 3-d scaled-up geostatistical reservoir models. In *SPE Annual Conference and Exhibition, Dallas*. Society of Petroleum Engineers, October 1995. SPE Paper Number 30570.

[14] J. J. Gómez-Hernández and A. G. Journel. Fast generation of grid-block permeabilities for the analysis of uncertainty on reservoir simulations. SPE paper # 22693, 1991.

[15] P. A. Gutteridge and D. E. Gawith. Connected volume calibration for well path ranking. In *European 3-D Reservoir Modelling Conference*, pages 197–206,

Stavanger, Norway, April 1996. Society of Petroleum Engineers. SPE paper # 35503.

[16] C. S. Horstmann and G. Cornell. *Core java: Volume I: Fundamentals.* Prentice Hall, 2000.

[17] C. S. Horstmann and G. Cornell. *Core java: Volume II: Advanced Features.* Prentice Hall, 2000.

[18] K. Hove, G. Olsen, S. Nilsson, M. Tonnesen, and A. Hatloy. From stochastic geological description to production forecasting in heterogeneous layered reservoirs. In *SPE Annual Conference and Exhibition, Washington, DC*, Washington, DC, October 1992. Society of Petroleum Engineers. SPE paper number 24890.

[19] C. D. G. Jr. and M. P. Vecchi. Optimization by simulated annealing. *Science*, pages 220(4598):671–680, May 1983.

[20] S. A. McKenna and E. P. Poeter. Simulating geological uncertainty with imprecise data for groundwater flow and advective transport modeling. In J. M. Yarus and R. L. Chambers, editors, *Stochastic Modeling and Geostatistics: Principles, Methods, and Case Studies*, pages 241–248. AAPG Computer Applications in Geology, No. 3, 1995.

[21] H. Omre, H. Tjelmeland, Y. Qi, and L. Hinderaker. Assessment of uncertainty in the production characteristics of a sandstone reservoir. In T. E. B. B. Linville and T. C. Wesson, editors, *Reservoir Characterization III*, pages 1–48. PennWell Books, 1993.

[22] A. Ouenes, S. Bhagavan, P. H. Bunge, and B. J. Travis. Application of simulated annealing and other global optimization methods to reservoir description: Myths and realities. In *SPE 69th Annual Conference and Exhibition, New Orleans,*

LA, pages 547–561, Washington, DC, September 1994. Society of Petroleum Engineers. SPE paper number 28415.

[23] M. N. Ponda and L. W. Lake. Parallel simulated annealing for stochastic reservoir modelling. In *68th Annual Technical Conference and Exhibition*, pages 23–31. Society of Petroleum Engineers, September 1993.

[24] W. H. Press, B. P. Flannery, S. a. Teukolsky, and W. T. Vetterling. *Numberical Recipes*. Cambridge University Press, New York, 1986.

[25] N. Saad, V. Maroongroge, and C. T. Kalkomey. Ranking geostatistical models using tracer production data. In *European 3-D Reservoir Modeling Conference*, Stavanger, Norway, April 1996. Society of Petroleum Engineers. SPE Paper Number 35494.

[26] M. G. Schlax. Application of simulated annealing. Research Notes / Personal Communication with Andre G. Journel, September 1985.

[27] D. Seifert, J. J. M. Lewis, C. Y. Hern, and N. C. T. Steel. Well placement optimisation and risking using 3-d stochastic reservoir modelling techniques. In *SPE/NPF European Conference*, Stavanger, Norway, April 1995. Society of Petroleum Engineers. SPE Paper Number 35520.

[28] K. Tyler, A. Henriquez, F. Georgsen, L. Holden, and H. Tjelmeland. A program for 3d modeling of heterogeneities in a fluvial reservoir. In *3rd European Conference on the Mathematics of Oil Recovery*, pages 31–40, Delft, June 1992.

[29] K. Tyler, T. Svanes, and A. Henriquez. Heterogeneity modelling used for production simulation or fluvial reservoir. *SPE Formation Evaluation*, pages 85–92, June 1992.

[30] S. Vasantharajan and A. S. Cullick. Well site selection uising integer programming. In V. Pawlowsky-Glahn, editor, *Proceedings of IAMG'97*, volume 1, pages 421–426. CIMNE, 1993.

[31] G. Vincent, B. Corre, and P. Thore. Managing structural uncertainty in a mature field for optimal well placement. 1999. SPE paper # 57468.

[32] B. Wang and C. V. Deutsch. Well site selection algorithm considering geologica, engineering and economic constraints: A progress report. Unpublished Research Notes:Centre for Computational Geostatistics Report Two: 1999/2000, MARCH 2000.

[33] B. Wang, C. V. Deutsch, and M. Al-Harbi. Well placement algorithm using geo-object connectivity of multiple realizations: Methodology and program. Unpublished Research Notes: Centre for Computational Geostatistics Report One: 1998/1999, MARCH 1999.